Neurobiology of Disease

Novel Dominant Rhodopsin Mutation Triggers Two Mechanisms of Retinal Degeneration and Photoreceptor Desensitization

Roustem Iakhine,[1]* **Irit Chorna-Ornan,**[2,4]* **Troy Zars,**[1] **Natalie Elia,**[3,4] **Yan Cheng,**[1] **Zvi Selinger,**[3,4] **Baruch Minke,**[2,4] **and David R. Hyde**[1,5]

[1]Department of Biological Sciences, University of Notre Dame, Notre Dame, Indiana 46556, and Departments of [2]Physiology and [3]Biological Chemistry and [4]Kühne Minerva Center for Studies of Visual Transduction, The Hebrew University, Jerusalem, Israel 91120

A variety of rod opsin mutations result in autosomal dominant retinitis pigmentosa and congenital night blindness in humans. One subset of these mutations encodes constitutively active forms of the rod opsin protein. Some of these dominant rod opsin mutant proteins, which desensitize transgenic *Xenopus* rods, provide an animal model for congenital night blindness. In a genetic screen to identify retinal degeneration mutants in *Drosophila*, we identified a dominant mutation in the *ninaE* gene (*NinaE*[PP100]) that encodes the rhodopsin that is expressed in photoreceptors R1–R6. Deep pseudopupil analysis and histology showed that the degeneration was attributable to a light-independent apoptosis. Whole-cell recordings revealed that the *NinaE*[PP100] mutant photoreceptor cells were strongly desensitized, which partially masked their constitutive activity. This desensitization primarily resulted from both the persistent binding of arrestin (ARR2) to the NINAE[PP100] mutant opsin and the constitutive activity of the phototransduction cascade. Whereas mutations in several *Drosophila* genes other than *ninaE* were shown to induce photoreceptor cell apoptosis by stabilizing a rhodopsin–arrestin complex, *NinaE*[PP100] represented the first rhodopsin mutation that stabilized this protein complex. Additionally, the *NinaE*[PP100] mutation led to elevated levels of $G_q\alpha$ in the cytosol, which mediated a novel retinal degeneration pathway. Eliminating both $G_q\alpha$ and arrestin completely rescued the *NinaE*[PP100]-dependent photoreceptor cell death, which indicated that the degeneration is entirely dependent on both $G_q\alpha$ and arrestin. Such a combination of multiple pathological pathways resulting from a single mutation may underlie several dominant retinal diseases in humans.

Key words: Drosophila; desensitization; photoreceptor; rhodopsin; dominant degeneration; arrestin; mutant

Introduction

Retinitis pigmentosa (RP) is a group of genetic disorders that exhibits abnormal electroretinograms and gradual vision loss attributable to the death of the rod and then cone photoreceptors in humans (Rattner et al., 1999; Phelan and Bok, 2000). Several X-linked and autosomal dominant and recessive forms of RP have been identified (Wang et al., 2001), with rhodopsin mutations being a prevalent cause of autosomal dominant RP (Kaushal and Khorana, 1994; Gal et al., 1997). Rhodopsin is a seven transmembrane, G-protein-coupled receptor that is activated by a photon of light to initiate the phototransduction cascade. Various models describe dominant rhodopsin-mediated

degeneration mechanisms, including the following: (1) defective maturation and/or trafficking of rhodopsin (Roof et al., 1994; Sung et al., 1994), (2) constitutively active rhodopsin and persistent stimulation of the phototransduction cascade (Robinson et al., 1992; Dryja et al., 1993; Rao et al., 1994), and (3) abnormal interactions between rhodopsin and the phototransduction components (Min et al., 1993; Li et al., 1995; Rim and Oprian, 1995).

The *Drosophila ninaE* gene encodes the rhodopsin protein (NINAE) that is expressed in six (R1–R6) of the eight adult photoreceptor cells in each ommatidium (O'Tousa et al., 1985; Zuker et al., 1985). The NINAE protein is activated by blue light, which stimulates the *dgq*-encoded $G_q\alpha$ subunit of the heterotrimeric G-protein (Lee et al., 1990, 1994; Scott et al., 1995). The photoactivated metarhodopsin is inactivated by phosphorylation and arrestin (ARR2) binding (Byk et al., 1993; Dolph et al., 1993; Kiselev and Subramaniam, 1994; Alloway and Dolph, 1999). Orange light photoconverts metarhodopsin to rhodopsin, which dissociates from arrestin and is dephosphorylated by the *rdgC*-encoded Ca^{2+}-dependent serine/threonine phosphatase (Byk et al., 1993). In the absence of arrestin dissociation, the persistent NINAE–arrestin complexes are endocytosed and induce apoptosis of photoreceptor cells (Alloway et al., 2000; Kiselev et al., 2000). Recessive *ninaE* mutants exhibit a defective light response

and photoreceptor cell death (Leonard et al., 1992). Dominant *ninaE* mutations were identified as suppressors of either *rdgC*-mediated (Kurada and O'Tousa, 1995) or *rdgB*-dependent (Colley et al., 1995) retinal degeneration. The *rdgB* gene encodes a novel phosphatidylinositol transfer protein that is required for the light response and photoreceptor viability (Vihtelic et al., 1991, 1993). All of the previously isolated dominant *ninaE* mutants are defective in the maturation and/or trafficking of rhodopsin in the endoplasmic reticulum (ER) (Colley et al., 1995; Kurada et al., 1998). Thus, dominant *ninaE* mutations likely mimic the degeneration mechanisms underlying rhodopsin-mediated autosomal dominant RP in humans.

We report a new dominant *ninaE* mutant ($NinaE^{PP100}$) that exhibits retinal degeneration and constitutively active and strongly desensitized photoreceptor cells. The photoreceptor cell desensitization and death resulted from both the NINAE^{PP100} mutant rhodopsin forming a stable complex with arrestin and the persistent localization of the $G_q\alpha$ in the cytosol. Genetic experiments reveal that the arrestin and $G_q\alpha$ mechanisms are mutually exclusive. Furthermore, the predominant localization of an active $G_q\alpha$ protein in the cytosol stimulates photoreceptor cell death through a novel mechanism.

Materials and Methods

Isolation of the dominant $NinaE^{PP100}$ mutant. Wild-type males were starved for 6 hr and then fed 25 mM ethyl methanesulfonate (Sigma, St. Louis, MO) in a 1% sucrose solution overnight (Lewis and Bacher, 1968). The males were mated en masse to *SM1/Sco; TM2/Sb* virgin females, and the F1 progeny were raised in constant light for 10 d. The F1 flies were screened for the absence of a wild-type deep pseudopupil, which is a virtual image of the rhabdomeres from several adjacent ommatidia (Franceschini, 1972).

Characterizing the retinal degeneration phenotype. Flies were raised under constant light and scored daily for the presence of the deep pseudopupil as described previously (Paetkau et al., 1999). The average percentage of flies possessing a wild-type deep pseudopupil and SDs were determined from at least four replicates (100–150 flies per trial) of each genotype and age. Flies raised in constant darkness were collected, aged until a designated day, scored for the presence or absence of a wild-type deep pseudopupil, and then discarded.

For light and electron microscopy of retinal sections, flies were raised in a 12 hr light/dark cycle to the desired age and then decapitated. The heads were bisected, fixed, and embedded in Polybed 812 as described previously (Lee et al., 1994). Sections for light and electron microscopy were generated and processed as described previously (Paetkau et al., 1999).

DNA isolation and sequencing. Genomic DNAs from wild-type and $NinaE^{PP100}$ mutant flies were isolated as described previously (Ashburner, 1989). Wild-type and mutant *ninaE* genes were PCR amplified using the 5′ A**GG ATC C**AA TGG AGA GGT ACG ATC GGT <u>GAA TCC</u> AC and 5′ GGT TGT **GGA TCC** AAA GAA TTT ATG CC primers that mapped to nucleotides −8 and 1518 of the *ninaE* gene, respectively (O'Tousa et al., 1985). Both PCR primers contain engineered *Bam*HI sites at their 5′ ends (in bold), and the first primer also deletes a *Bam*HI site (underlined) in the first *ninaE* intron. The PCR reactions contained 3 μg of genomic DNA, 1× native *Pfu* buffer, 2.5 mM of each dNTP, and 250 pmol of each primer. After incubating at 96°C for 7 min, 1 μl of native *Pfu* DNA polymerase (Stratagene, La Jolla, CA) was added and amplified through 30 cycles of 96°C for 1 min, 54°C for 1 min, and 72°C for 4 min, followed by a 10 min extension at 72°C. The PCR products were size fractionated on a Tris acetate-EDTA agarose gel, purified with the Wizard PCR prep resin (Promega, Madison, WI), and blunt-end ligated into the pZero 2.1 vector (Invitrogen, Carlsbad, CA). The plasmid DNA was purified with Stratclean Resin (Stratagene), precipitated, resuspended in H_2O, and sequenced using the Sequenase Quick Denature Kit (US Biochemicals, Cleveland, OH), with primers generated from the published *ninaE* genomic sequence (O'Tousa et al., 1985).

In vitro mutagenesis. The *Pfu*-generated wild-type *ninaE* gene was digested from pZero 2.1 with *Bam*HI, gel purified, and cloned into the *Bam*H1 site of the PK− ATG− vector, which contains the 3.2 kb *ninaE* promoter and a 0.7 kb *ninaE* poly(A^+) tail (Kurada and O'Tousa, 1995; Shetty et al., 1998). The $NinaE^{PP100}$ mutation was introduced into the wild-type *ninaE* gene by *in vitro* mutagenesis in the PK− ATG− vector using the Quick Change Site-Directed Mutagenesis kit (Stratagene) and the complementary primer pairs 5′ TCA ACT GCA TG**A** GAC TGT TCA AGT 3′ and 5′ ACT GGA ACA GTC T**CA** TGC AGT TGA 3′ (the site of the nucleotide change is in bold). The PCR reaction contained 50 ng of template DNA, 125 ng of each primer, 1× buffer, 10 mM of each dNTP, and 1 μl of *Pfu* DNA polymerase. The PCR amplification protocol was 95°C for 30 sec and then 12 cycles of 95°C for 30 sec, 60°C for 1 min, 68°C for 2 min, and a final 15 min extension at 68°C.

Germ-line transformation. A 5.4 kb *Kpn*I fragment containing the *ninaE* promoter, the *in vitro* mutagenized *ninaE* genomic DNA, and the *ninaE* poly(A^+) tail was gel purified and cloned into the *Kpn*I site of the pCaSpeR-4 transformation vector (Ashburner, 1989). The sequence of the entire *ninaE* coding region was confirmed in this vector. This *in vitro* mutagenized DNA was germ-line transformed with the Δ2–3 P-element (ratio of 6:1) using standard techniques (Spradling, 1986).

Electrophysiology. Electroretinograms (ERGs) were performed as described previously (Paetkau et al., 1999). ERG traces were recorded using a MacAdios II analog-to-digital converter using SuperScope II software on a Macintosh IIx computer (Apple Computers, Cupertino, CA).

To measure light-induced currents (LICs), orange light (OG 590 Ditric edge filter) from a xenon high-pressure lamp (75 W) was delivered to isolated ommatidia via the objective lens (60× Olympus Optical, Tokyo, Japan) and attenuated up to seven orders of magnitude by neutral density filters. The maximal luminous intensity of the orange light at the level of the ommatidia was ~3.0 log units above the intensity required for a half-maximal response of the R1–R6 photoreceptors. The effective intensity of the white light without the orange filter was determined by comparing the light intensities with and without the orange filter, which were required to elicit a small response of the same amplitude in wild-type flies. In Figure 4, the intensity of the white light stimulus was converted to the effective relative intensity of orange light.

Dissociated ommatidia were prepared from either newly eclosed adult flies (<1 hr after eclosion) or late pupae as described previously (Hardie, 1991). Whole-cell patch-clamp recordings were performed as described previously (Hardie and Minke, 1992; Peretz et al., 1994). Recordings were made at 21°C using patch pipettes of 5–10 MΩ pulled from fiber-filled borosilicate glass capillaries. Series resistance of 7–14 MΩ was carefully compensated (>80%) during all experiments. Signals were amplified with an Axopatch-1D or 2B (Axon Instruments, Foster City, CA) patch-clamp amplifier, sampled at 2 kHz, and filtered below 1 kHz.

Immunoblots of NINAE, ARR2, and $G_q\alpha$ proteins. Immunoblots of rhodopsin expression in flies 4–6 hr old were performed as described previously (Milligan et al., 1997). Head protein homogenates were electrophoresed, electrotransferred to Hybond polyvinylidene difluoride (PVDF) membrane (Amersham Biosciences, Piscataway, NJ), and incubated with the 4C5 anti-rhodopsin monoclonal antibody (Developmental Studies Hybridoma Bank, University of Iowa, Iowa City, IA). The 4C5 monoclonal antibody was detected with HRP-conjugated goat anti-mouse antibodies (1:5000) and ECL reagents (Amersham Biosciences). Band intensity was quantified on a scanning laser densitometer (Bio-Rad, Hercules, CA) and normalized to a standard curve generated by a dilution series of head protein extract, with five independent blots analyzed.

The ARR2 protein was isolated under dim red light from white-eyed wild-type and mutant fly heads that were 4 hr after eclosion. The heads were placed in 20 μl of PBS, pH 7.4, illuminated at the desired wavelength for 2 min, homogenized in darkness, and centrifuged with 15,000 × *g*. The supernatant fraction was transferred to a new Eppendorf tube (Eppendorf Scientific, Westbury, NY), and the pellet was resuspended in 20 μl of PBS. SDS extraction buffer (20 μl) was added to both fractions and incubated at 45°C for 1 hr before electrophoresing one head equivalent of cytosolic and membrane protein extracts through a 7–15% gradient SDS-PAGE gel. After electrotransfer, the PVDF membranes were incu-

bated with a mixture of the 4C5 anti-rhodopsin monoclonal antibody and anti-ARR2 rabbit polyclonal antisera (Alloway et al., 2000; Kiselev et al., 2000) and detected with a mixture of HRP-conjugated mouse anti-rabbit and rabbit anti-mouse antibodies and the ECL system (Amersham Biosciences), with five independent blots analyzed.

The $G_q\alpha$-protein was quantitated in different subcellular fractions as described previously (Kosloff et al., 2003). Wild-type and $NinaE^{pp100}$ flies were dark adapted for 24 hr and then subjected to either blue light illumination (490 nm) or continued darkness for 10 min at 22°C. The heads were homogenized at 4°C in the dark in hypotonic medium (20 mM HEPES buffer, pH 7.6, containing 15 mM *N*-ethylmaleimide, 20 μg/ml leupeptin, 1 μg/ml pepstatin A, and 0.35 mg/ml *o*-phenanthroline). The samples were centrifuged at $15{,}800 \times g$ for 15 min at 4°C to separate the membrane pellet from the soluble proteins. The pellet was washed and centrifuged, and the supernatants were combined. Ultracentrifugation at $150{,}000 \times g$ for 30 min did not change the $G_q\alpha$ distribution between the fractions. The proteins were precipitated in 5% TCA, electrophoresed on a 10% SDS-PAGE, and electrotransferred to nitrocellulose using a semidry transfer apparatus (Bio-Rad). The nitrocellulose was blocked and incubated with a rabbit anti-$G_q\alpha$ polyclonal antibody raised against the decapeptide of the C terminus of the protein. The nitrocellulose was incubated with anti-rabbit polyclonal antiserum and detected with ECL Amersham Biosciences reagents according to the instructions of the manufacturer and quantitated with Fuji LAS-1000. The amount of $G_q\alpha$ in each fraction was calculated as a percentage of the total $G_q\alpha$ in the pellet and supernatant, with four independent blots analyzed.

GTPase assay. GTP hydrolysis of *Drosophila* head extracts under various light conditions were performed essentially as described previously (Blumenfeld et al., 1985).

Results

The $NinaE^{pp100}$ mutant exhibits a dominant retinal degeneration and a recessive electrophysiological defect

In a screen to identify *Drosophila* mutants that lacked a deep pseudopupil, we identified a dominant retinal degeneration mutation that mapped <1 cM from the *ninaE* gene, which encodes the rhodopsin protein expressed in photoreceptor cells R1–R6 (O'Tousa et al., 1985; Zuker et al., 1985). To determine whether $NinaE^{pp100}$ was a *ninaE* allele, we examined the ERGs of flies that were ~12 hr after eclosion (before any signs of degeneration). White-eyed wild-type flies exhibited a prolonged depolarizing afterpotential (PDA) after a blue light converts a large fraction of rhodopsin to metarhodopsin (Fig. 1*A*) (Hillman et al., 1983; Dolph et al., 1993). The white-eyed $ninaE^{I17}/ninaE^{I17}$ null mutant lacked a PDA and possessed small light response amplitudes (Fig. 1*B*), which were attributable to the opsins expressed in photoreceptor cells R7 and R8. White-eyed $NinaE^{pp100}/ninaE^{+}$ flies exhibited a wild-type ERG light response and a PDA (Fig. 1*C*), whereas $NinaE^{pp100}/NinaE^{pp100}$ flies lacked the PDA (Fig. 1*E*). Thus, the $NinaE^{pp100}$ flies exhibited a recessive mutant ERG phenotype. White-eyed $NinaE^{pp100}/ninaE^{I17}$ flies also lacked the PDA (Fig. 1*D*), which confirmed that $NinaE^{pp100}$ was a *ninaE* allele.
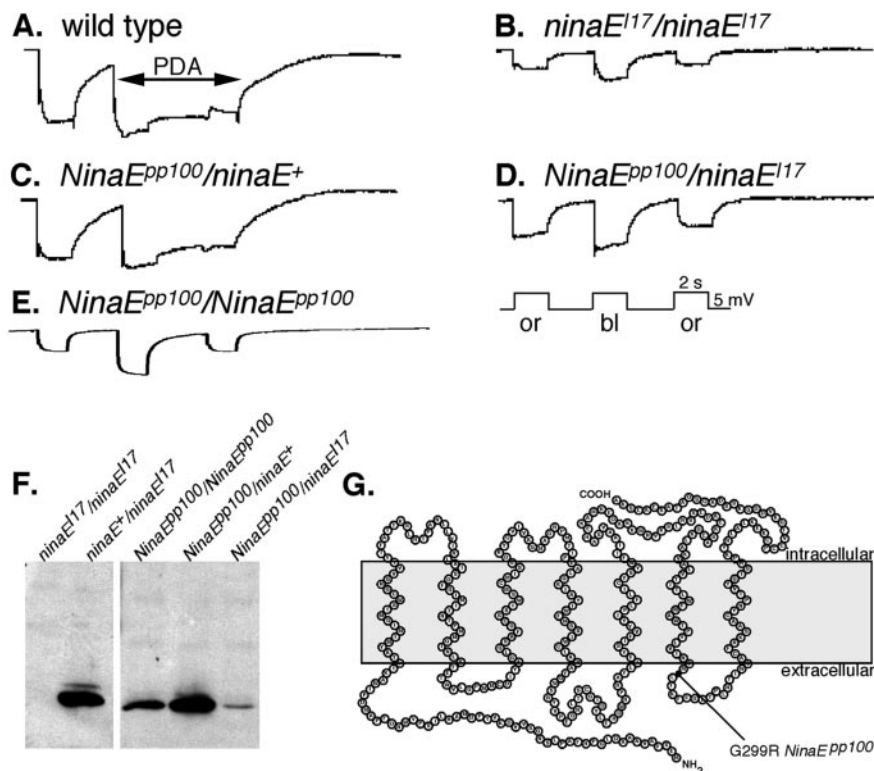

Figure 1. $NinaE^{pp100}$ is a *ninaE* allele. We recorded the ERG light response of wild-type (*A*), $ninaE^{I17}/ninaE^{I17}$ (*B*), $NinaE^{pp100}/ninaE^{+}$ (*C*), $NinaE^{pp100}/ninaE^{I17}$ (*D*), and $NinaE^{pp100}/NinaE^{pp100}$ (*E*) flies at ~12 hr after eclosion. Each fly was stimulated for 2 sec with orange light (or), 2 sec with blue light (bl), and a final 2 sec with orange light, as shown below *D*. Wild-type flies exhibited a PDA in response to blue light (*A*, *C*), which was absent in *ninaE* mutant flies (*B*, *D*, *E*). Calibration for ERG responses is shown below *D*. *F*, Immunoblot of rhodopsin expression relative to wild-type flies for $ninaE^{I17}/ninaE^{I17}$ flies (undetectable), $ninaE^{+}/ninaE^{I17}$ heterozygotes (62% ± 4%), $NinaE^{pp100}/NinaE^{pp100}$ flies (21% ± 5.0%), $NinaE^{pp100}/ninaE^{+}$ flies (75% ± 4.7%), and $NinaE^{pp100}/ninaE^{I17}$ flies (12% ± 3.1%). *G*, The putative amino acid sequence of the NINAE opsin protein is shown as a single letter amino acid code. The N and C termini are labeled (NH2 and COOH, respectively), with the relative orientation of the intracellular and extracellular faces of the membrane labeled. The NINAE^{pp100} mutation (G299R) is shown.

Immunoblots revealed that the $NinaE^{pp100}$ mutant gene expressed ~20% of the rhodopsin relative to the $ninaE^{+}$ gene (Fig. 1*F*). We sequenced the *ninaE* gene from the $NinaE^{pp100}$ mutant and identified a G-to-A transition mutation, which changed the glycine at amino acid 299 to arginine (Fig. 1*G*).

We examined the retinal degeneration that underlies the deep pseudopupil loss in the $NinaE^{pp100}$ mutant. A 2-d-old wild-type retina possessed a regular repeating pattern of ommatidia (Fig. 2*A*, left column), whereas the ultrastructure of a 10-d-old retina revealed large R1–R6 rhabdomeres surrounding the central R7 rhabdomere (Fig. 2*A*, right column). In contrast, the 2-d-old $NinaE^{pp100}/ninaE^{+}$ retina possessed a few holes and reduced or missing rhabdomeres (Fig. 2*B*). Electron microscopy of the 10-d-old $NinaE^{pp100}/ninaE^{+}$ retina revealed degenerating R1–R6 photoreceptors (darkly stained) and phagocytosed photoreceptors (Fig. 2*B*, asterisks). To prove that the G299R mutation caused the dominant $NinaE^{pp100}$ mutant phenotype, we created three independent transgenic lines that contained a wild-type *ninaE* gene that was *in vitro* mutagenized to introduce the G299R mutation. At both the light and electron microscope level, all three transgenic lines ($ninaE^{+}$, *P[ninaE-G299R]/ninaE^{I17}$) (Fig. 2*C*) exhibited a dominant degeneration phenotype that was indistinguishable from the $NinaE^{pp100}/ninaE^{+}$ flies. Therefore, the G299R mutation accounted for the dominant $NinaE^{pp100}$ degeneration phenotype.

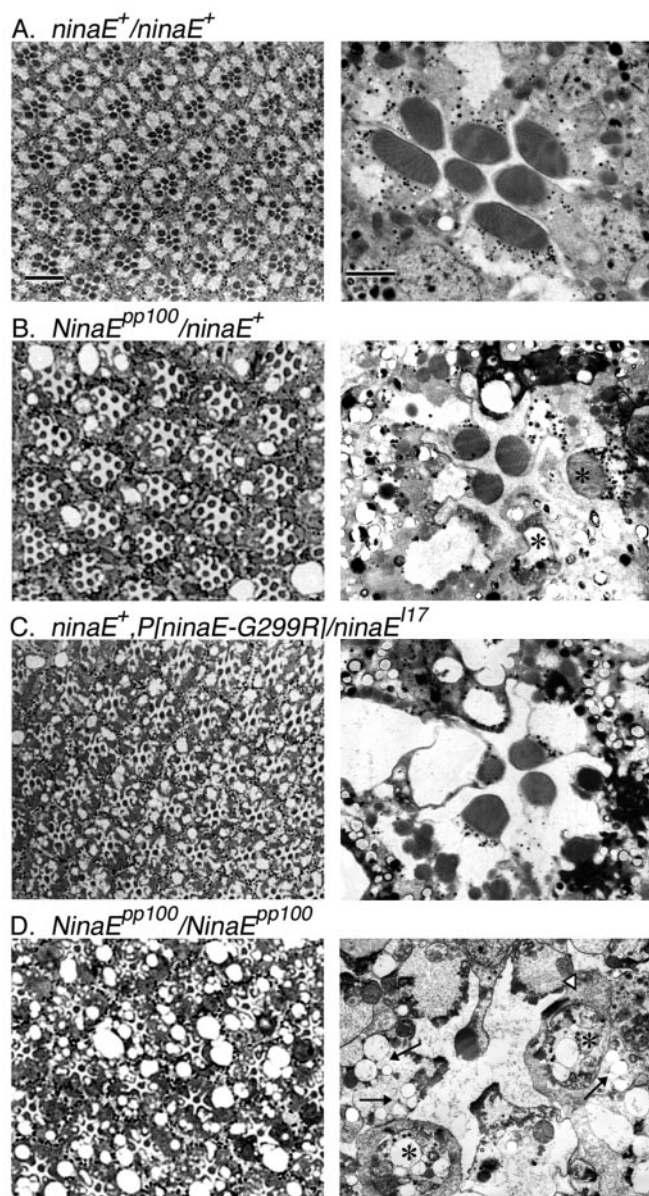Because the $NinaE^{pp100}$ mutant exhibited a recessive ERG light

Figure 2. The $NinaE^{pp100}$ retinal degeneration phenotype. The histology of wild-type ($ni-naE^+/ninaE^+$; A), $NinaE^{pp100}/ninaE^+$ (B), $ninaE^+$, $P[ninaE-G299R]/ninaE^{I17}$ transgenic flies (C), and $NinaE^{pp100}/NinaE^{pp100}$ flies (D) were examined using light microscopy (2 d after eclosion; left column) and electron microscopy (10 d after eclosion; right column). The dominant $NinaE^{pp100}$ (B) degeneration phenotype was characterized by loss of rhabdomeres, presence of intracellular vacuoles, and phagocytosis of photoreceptors (asterisks). The transgenic flies (C) exhibited a degeneration that was indistinguishable from the dominant mutant phenotype, which confirmed that the G299R mutation caused the dominant degeneration. The homozygous $NinaE^{pp100}$ degeneration (D) was characterized by a rapid loss of the rhabdomeres, increased number of large intracellular vesicles (arrows), phagocytosis of the photoreceptor cells (asterisk), and cytoplasmic condensation (arrowhead). Scale bars (in A): left, 10 μm; right, 1 μm (shown in the wild-type sections and are the same for the subsequent sections).

response defect, we examined the histology of $NinaE^{pp100}$ homozygotes. The 2-d-old $NinaE^{pp100}/NinaE^{pp100}$ retina exhibited an increased number of large intracellular vesicles, more ommatidial disorganization, and fewer rhabdomeres relative to $Nina-E^{pp100}/ninaE^+$ (Fig. 2D,B, respectively). The ultrastructure of a 10-d-old $NinaE^{pp100}/NinaE^{pp100}$ ommatidium revealed that the R1–R6 rhabdomeres were more disorganized and smaller than the central R7 rhabdomere, and many large intracellular vesicles (Fig. 2D, arrows) were present within some of the R1–R6 photo-
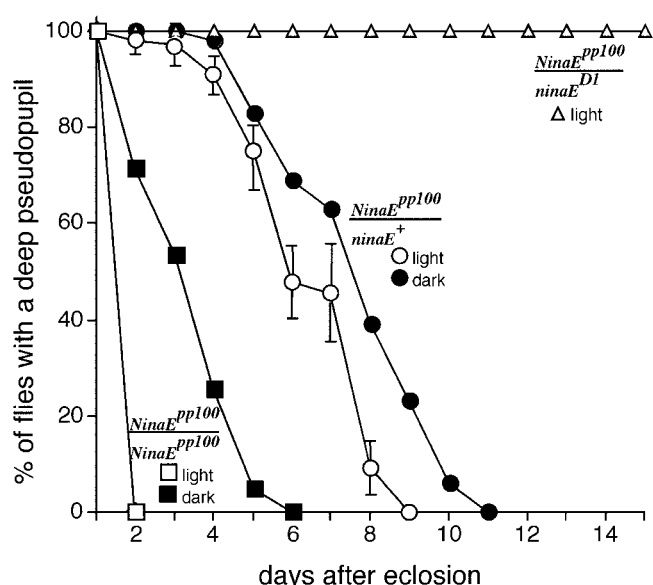

Figure 3. Rates of $NinaE^{pp100}$ deep pseudopupil loss. We examined the time course of deep pseudopupil loss of $NinaE^{pp100}/NinaE^{pp100}$ flies (squares), $NinaE^{pp100}/ninaE^+$ flies (circles), and $NinaE^{pp100}/ninaE^{D1}$ flies (triangles) under constant light and constant darkness (open and filled symbols, respectively). The homozygous $NinaE^{pp100}$ mutants exhibited an earlier and more rapid deep pseudopupil loss relative to the heterozygous $NinaE^{pp100}$ mutants. Furthermore, both the homozygous and heterozygous $NinaE^{pp100}$ mutants exhibited more rapid deep pseudopupil loss in constant light relative to constant darkness. The $ninaE^{D1}$ mutation strongly suppressed the rapid $NinaE^{pp100}$ deep pseudopupil loss (triangles). The percentages of flies retaining a deep pseudopupil on each day were plotted against their age, with each symbol representing the average from four independent trials of 100–150 flies per trial.

receptors. Some photoreceptors were being phagocytosed, and others exhibited a decreased cytoplasmic volume (Fig. 2D, asterisks, arrowhead, respectively). Thus, the $NinaE^{pp100}$ mutation caused a dominant retinal degeneration that was enhanced in the $NinaE^{pp100}$ homozygote.

The $NinaE^{pp100}$ mutant exhibits a light-enhanced retinal degeneration

We examined the effect of light on the $NinaE^{pp100}$ retinal degeneration to differentiate between various potential degeneration mechanisms. We used the deep pseudopupil as a rapid and noninvasive technique to assay the integrity of the retina and photoreceptor cells (Franceschini, 1972). The $NinaE^{pp100}$ mutant exhibited a dominant deep pseudopupil loss that was slightly faster in constant light than in constant darkness (Fig. 3, $NinaE^{pp100}/ninaE^+$, open circles, filled circles, respectively). The absence of any wild-type NINAE$^+$ protein in the $NinaE^{pp100}/NinaE^{pp100}$ flies dramatically increased the onset and rate of deep pseudopupil loss relative to $NinaE^{pp100}/ninaE^+$ (Fig. 3). Furthermore, the $Ni-naE^{pp100}/NinaE^{pp100}$ degeneration time course exhibited a significantly faster deep pseudopupil loss in constant light relative to constant darkness (Fig. 3, open squares, filled squares, respectively). The $NinaE^{pp100}/ninaE^{I17}$ flies exhibited a deep pseudopupil loss that mimicked the $NinaE^{pp100}/NinaE^{pp100}$ degeneration time course (data not shown). The $ninaE^{D1}$ mutation, which is a serine-to-phenylalanine change at position 137 in the third transmembrane domain, causes a slow dominant retinal degeneration by blocking rhodopsin maturation in the endoplasmic reticulum (Kurada and O'Tousa, 1995; Kurada et al., 1998). The $ninaE^{D1}$ mutation suppressed the rapid $NinaE^{pp100}$-dependent deep pseudopupil loss (Fig. 3, $NinaE^{pp100}/ninaE^{D1}$, triangles). Therefore,

the $NinaE^{PP100}$ mutation must cause its rapid degeneration through a mechanism subsequent to the $ninaE^{D1}$ block of rhodopsin maturation in the ER (Kurada and O'Tousa, 1995).

The $NinaE^{PP100}$ mutant is strongly desensitized

We performed whole-cell recordings on the homozygous $NinaE^{PP100}$ mutant before photoreceptor degeneration to elucidate the underlying physiological defect. The wild-type LIC to dim orange light stimulus showed current fluctuations that are attributable to the summation of the quantum bumps (Fig. 4A, top left panel), whereas a bright orange light stimulus invoked an initial transient phase that declined to a small steady-state phase attributable to light adaptation (Fig. 4A, top right panel). The LIC from one of the most sensitive $NinaE^{PP100}$ mutant cells to intense orange light elicited only a small response that lacked large current fluctuations (Fig. 4A, middle left panel). Furthermore, the intense white light required to elicit a sizable response in the $NinaE^{PP100}$ mutant (Fig. 4A, middle right panel) was approximately four orders of magnitude brighter than the stimulus eliciting a similar response amplitude in a wild-type cell. The need for a more intense light stimulus to induce a wild-type-sized LIC response in $NinaE^{PP100}$ suggested that the $NinaE^{PP100}$ mutant possessed a highly reduced sensitivity to light. The individual $NinaE^{PP100}$ cells exhibited a large variability in their sensitivity to light, with only a fraction of the light-sensitive $NinaE^{PP100}$ mutant cells possessing the maximal peak response amplitude (data not shown). Because this amplitude was similar to that of wild-type flies, the mutant cells must contain a sufficient number of light-sensitive rhodopsin molecules. It was shown previously that the high gain of the phototransduction cascade resulted in the $ninaE^{P332}$ mutant exhibiting a shift of ~3.5 orders of magnitude in the intensity–response function (V-log I curve) and a wild-type peak amplitude of the receptor potential, although it had approximately three orders of magnitude less rhodopsin than wild-type flies (Johnson and Pak, 1986).

To confirm the reduced light sensitivity of the $NinaE^{PP100}$ cells, we plotted the intensity–response function (i-log I curve) for several different individual $NinaE^{PP100}$ mutant and wild-type cells (Fig. 4B). There was a large difference in the light intensity range at which wild-type and the $NinaE^{PP100}$ photoreceptors responded, with a considerable fraction of mutant cells either not responding to the maximal white light intensity or only exhibiting minimal response amplitudes. This data clearly demonstrated that a main electrophysiological phenotype of the $NinaE^{PP100}$ mutant relative to wild type is a large decrease in the sensitivity to light.

The $NinaE^{PP100}$ desensitization is partially rescued by elimination of arrestin

One mechanism that could underlie the $NinaE^{PP100}$ reduced light sensitivity is persistent binding of arrestin (ARR2) to NINA-E^{PP100}. Persistent arrestin binding was shown previously to result in retinal degeneration of several *Drosophila* mutants (Alloway et al., 2000; Kiselev et al., 2000) and the transgenic mouse model expressing the K296E mutant human opsin (Li et al., 1995). Whole-cell recordings on the $arr2^{Y20STOP}$ $NinaE^{PP100}$ double mutant (Fig. 4A, bottom left panel) revealed the bump noise that was also observed in wild-type flies (Fig. 4A, top left panel), but absent in $NinaE^{PP100}$ (Fig. 4A, middle left panel). Although the $arr2^{Y20STOP}$ $NinaE^{PP100}$ double mutant revealed a large increase in light sensitivity relative to $NinaE^{PP100}$, it was still significantly less sensitive than wild type (Fig. 4A, bottom right panel). We compared the intensity–response function (i-log I curve) of the
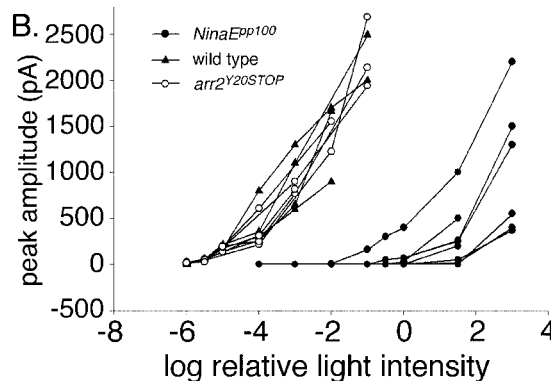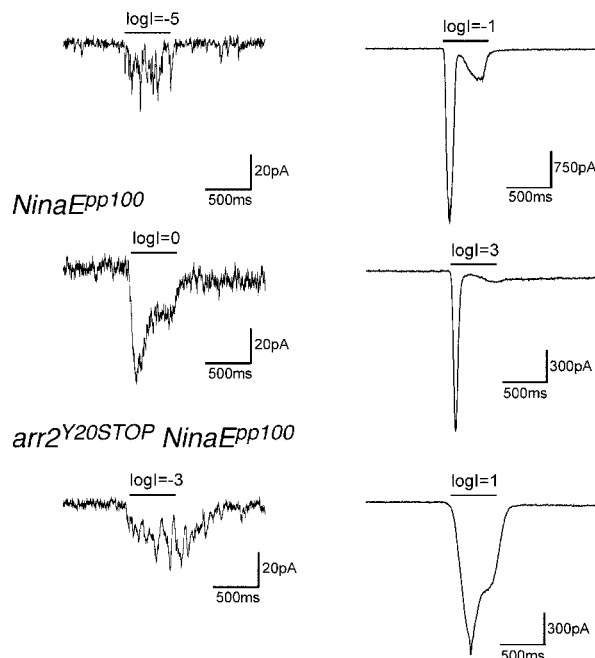

Figure 4. LICs of $NinaE^{PP100}$ mutants exhibit a highly reduced sensitivity to light relative to wild-type flies. *A*, Top row, LIC of a wild-type photoreceptor cell in response to dim (log I = −5.0) and more intense (log I = −1.0) orange light pulses indicated by horizontal bars. The response to the dim light shows the typical current fluctuations attributable to the summation of quantum bumps. The response to intense light shows the initial transient phase that declines to a small steady-state phase attributable to light adaptation. Note the different current scales below all of the responses. *A*, Middle row, LIC of a $NinaE^{PP100}$ photoreceptor cell in response to intense orange light (log I = 0) and more intense white light expressed in equivalent orange light intensity (log I = 3). No bump noise is observed. *A*, Bottom row, LIC of an $arr2^{Y20STOP}$ $NinaE^{PP100}$ photoreceptor cell in response to medium intensity orange light (log I = −3) and more intense white light expressed in equivalent orange light intensity (log I = 1). Note the appearance of bump noise at the lower light intensity. The slower LIC waveforms at both light intensities are typical for the $arr2$ mutant phenotype. *B*, Families of intensity–response functions (i-log I curves) obtained from wild-type, $NinaE^{PP100}$, and $arr2^{Y20STOP}$ mutant photoreceptors. The graph plots the peak current amplitudes of the responses (in picoamperes) for wild-type (filled triangles), $NinaE^{PP100}$ (filled circles), and $arr2^{Y20STOP}$ (open circles) mutant photoreceptors. Only a few of the $NinaE^{PP100}$ mutant cells responded to the intense orange light stimulus. The light intensity range above log I = 0 was obtained with white light that was converted to equivalent orange intensity (see Materials and Methods). The $arr2^{Y20STOP}$ cells possessed i-log I curves that were indistinguishable from wild type.

$arr2^{Y20STOP}$ mutant photoreceptors with wild-type and $NinaE^{PP100}$ cells and found that the family of $arr2^{Y20STOP}$ responses was nearly identical to wild type (Fig. 4B). Thus, the ARR2 protein specifically interacted with the NINAE^{PP100} mutant rhodopsin to decrease the sensitivity to light. However, this interaction failed
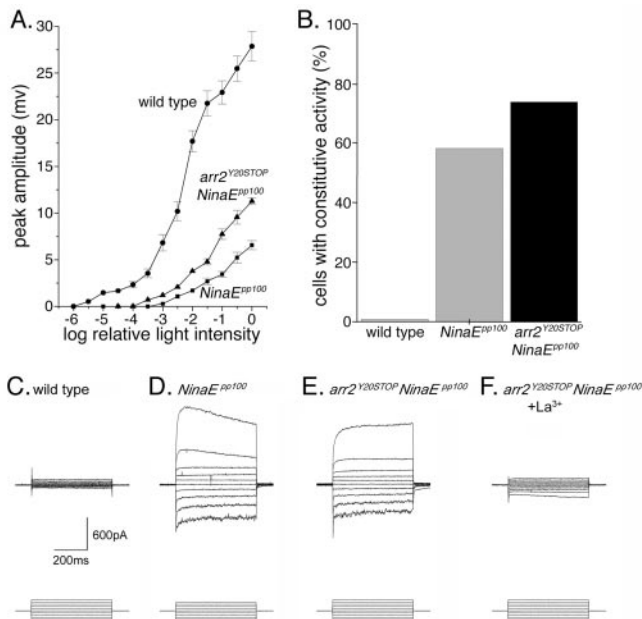
Figure 5. The *NinaE^{pp100}* mutation induces constitutive activity of the light-sensitive channels. *A*, *In vivo* ERG recordings of intensity–response functions measured in wild-type (filled circles; $n = 6$), *NinaE^{pp100}* (filled squares; $n = 8$), and *arr2^{Y20STOP} NinaE^{pp100}* (filled triangles; $n = 6$). The *arr2^{Y20STOP}* mutation increased the *NinaE^{pp100}* sensitivity to light ~10-fold. *B*, Histograms plotting the percentage of *NinaE^{pp100}* ($n = 33$ adult flies and 10 pupae) and *arr2^{Y20STOP} NinaE^{pp100}* ($n = 23$, all pupae) cells showing constitutive activity in the dark. The *arr2^{Y20STOP}* mutation increased the fraction of *NinaE^{pp100}* cells exhibiting constitutive activity. *C–F*, Families of current traces elicited by a series of 20 mV voltage steps from −100 to +80 mV (bottom row). A wild-type photoreceptor in the dark exhibits only a small leak current (*C*). Both *NinaE^{pp100}* and *arr2^{Y20STOP} NinaE^{pp100}* pupal photoreceptors possess inward and outward rectifying currents in the dark (*D*, *E*, respectively). Addition of 20 μM La^{3+} to the external medium of the same *arr2^{Y20STOP} NinaE^{pp100}* pupal cell almost completely abolished the current (*F*). Very similar results were obtained when adult (newly eclosed) flies were used, except that, at negative holding potentials, the inward currents were smaller. Calibration is shown under the wild-type traces (*C*) and is the same for *D–F*.

to account for the entire range of reduced sensitivity of the *NinaE^{pp100}* cells.

We extended this analysis by plotting the peak amplitude versus log of the relative light intensity from *in vivo* ERG recordings and confirmed that the *arr2^{Y20STOP} NinaE^{pp100}* double mutant possessed an increased light sensitivity relative to the *NinaE^{pp100}* mutant (Fig. 5*A*). Although these observations strongly suggested that arrestin contributed to the reduced light sensitivity of the *NinaE^{pp100}* mutant, Figures 4*A* (bottom row) and 5*A* revealed that the *arr2^{Y20STOP} NinaE^{pp100}* double mutant remained less sensitive to light relative to wild-type flies. This remaining desensitization in the *arr2^{Y20STOP} NinaE^{pp100}* fly may be attributable to either the NINAE^{PP100} molecules being constitutively active or a reduced interaction between NINAE^{PP100} and the heterotrimeric G-protein.

To investigate whether the NINAE^{PP100} molecules were constitutively active and induced persistent opening of the light-activated channels, we recorded whole-cell membrane currents to voltage steps in the dark (Fig. 5*C–F*). Wild-type cells revealed no significant currents under these conditions (Fig. 5*C*). However, small but significant (Yoon et al., 2000) currents were recorded from both *NinaE^{pp100}* and *arr2^{Y20STOP} NinaE^{pp100}* mutant cells (Fig. 5*D,E*, respectively). The characteristics of these currents and their ability to be blocked by a low concentration of La^{3+} (Fig. 5*F*) suggested that they originate from constitutively open transient receptor potential (TRP) channels (Hardie and

Minke, 1994), which are the major light-activated channels (for review, see Minke and Hardie, 2000). These constitutive currents were recorded in 58% of the *NinaE^{pp100}* cells and 74% of the *arr2^{Y20STOP} NinaE^{pp100}* double mutant photoreceptors (Fig. 5*B*). Because the *arr2^{Y20STOP}* mutant cells failed to exhibit any significant whole-cell membrane currents to voltage steps in the dark (data not shown), the *arr2^{Y20STOP}* mutation only contributed to the constitutive opening of the TRP channels in the presence of the NINAE^{PP100} mutant rhodopsin (Fig. 5*B*). Although arrestin partially masked the production of the constitutive current, possibly through a stable NINAE^{PP100}–ARR2 complex, it is not clear why some of the mutant cells were not constitutively active. This may be related to variability in the level of rhodopsin among different *NinaE^{pp100}* cells, which is consistent with the large variability in the light sensitivity between different *NinaE^{pp100}* mutant cells (Fig. 4*B*).

The dominant *NinaE^{pp100}* mutant requires both G$_q\alpha$ and ARR2 proteins for rapid degeneration

It was shown previously that the *norpA*, *rdgB*, and *rdgC* mutations produced a persistent NINAE–ARR2 complex that induced photoreceptor cell apoptosis (Alloway et al., 2000; Kiselev et al., 2000). Because the electrophysiology suggested that a stable NINAE^{PP100}–ARR2 complex was present, we examined whether loss of the ARR2 protein suppressed the rapid *NinaE^{pp100}*-dependent degeneration. At 10 d after eclosion, wild-type photoreceptors possessed large rhabdomeres (Fig. 6*A*), whereas a 4-d-old *NinaE^{pp100}* mutant possessed significantly smaller and disorganized rhabdomeres and signs of photoreceptor cell death (Fig. 6*D*). The *arr2^{Y20STOP}* null mutant possessed slightly smaller and irregular-shaped rhabdomeres relative to wild type (Fig. 6*B*), which is consistent with the light-dependent deep pseudopupil loss described previously (Alloway and Dolph, 1999). The 4-d-old *arr2^{Y20STOP} NinaE^{pp100}* double mutant also exhibited small and abnormally shaped rhabdomeres (Fig. 6*E*), similar to the *arr2^{Y20STOP}* mutant. However, neither *arr2^{Y20STOP}* nor *arr2^{Y20STOP} NinaE^{pp100}* exhibited the massive rhabdomere loss and photoreceptor cell death that occurred in the *NinaE^{pp100}* mutant. This suggested that a stable NINAE^{PP100}–ARR2 complex induced both photoreceptor desensitization and cell death. Furthermore, the time course of deep pseudopupil loss revealed that the *arr2^{Y20STOP}* mutation significantly slowed, but did not abolish, the *NinaE^{pp100}* degeneration in both constant light and constant darkness (data not shown). Thus, the NINAE^{PP100}–ARR2 complex was not the sole cause of retinal degeneration, and an additional independent mechanism must participate in generating the *NinaE^{pp100}* mutant phenotypes.

Because the electrophysiology revealed that the NINAE^{PP100} mutant protein was constitutively active, we examined whether activation of the light-sensitive channels induced the retinal degeneration phenotype. It was demonstrated previously that the early-onset retinal degeneration in the *rdgA^{BS12}* mutant, which possesses constitutively active light-sensitive channels, was significantly slowed by the *trp^{301}* mutation (Raghu et al., 2000). We examined whether mutants blocking three different points in the phototransduction cascade could suppress the rapid *NinaE^{pp100}*-dependent degeneration. The mutations we tested corresponded to the *dgq* (which encodes the G$_q\alpha$ that is stimulated by light-activated metarhodopsin), *norpA* (which encodes the phospholipase C that is activated by G$_q\alpha$), and *trp* genes (which encodes the major light-activated channel). The *norpA^{p24}* mutant exhibited no signs of retinal degeneration when raised for 6 d in constant darkness (Fig. 7*B*). In contrast, the *NinaE^{pp100}* mutant pos-

sessed the previously described degeneration phenotype after 6 d in constant darkness (Fig. 7C). Although *norpA^{P24}; NinaE^{PP100}* exhibited reduced and misshapen rhabdomeres after 6 d in constant darkness (Fig. 7D), it lacked the severe degeneration that was present in the *NinaE^{PP100}* mutant. This suggests that *norpA^{P24}* slightly delayed the *NinaE^{PP100}* degeneration. Similarly, the *trp^{301}* mutation only slightly suppressed *NinaE^{PP100}* degeneration relative to the *arr2^{Y20STOP}* mutation (Fig. 7E). Thus, constitutive activation of the phototransduction cascade is only a minor component of the *NinaE^{PP100}* degeneration mechanism.

Surprisingly, a mutation in the *dgq* gene, which encodes the $G_q\alpha$ subunit target for metarhodopsin (Lee et al., 1990, 1994; Scott et al., 1995), suppressed the *NinaE^{PP100}* deep pseudopupil loss substantially better than the *trp^{301}* mutation (Figs. 6K, 7E, respectively). At 10 d after eclosion, the *dgq^1* mutant possessed only a few missing rhabdomeres relative to the massive rhabdomere loss and photoreceptor cell death in *NinaE^{PP100}* (Fig. 6C,D, respectively). The ultrastructure of a 10-d-old *dgq^1; NinaE^{PP100}* double mutant exhibited only minor photoreceptor abnormalities that were similar to the *dgq^1* mutant (Fig. 6F,C, respectively). Furthermore, the time course of deep pseudopupil loss in the *dgq^1; NinaE^{PP100}* double mutant was similar to the *dgq^1* mutant in both dark and light-raised flies, which was significantly slower than the *NinaE^{PP100}* mutant (Fig. 6K). However, both the *dgq^1; NinaE^{PP100}* and *arr2^{Y20STOP} NinaE^{PP100}* double mutants still exhibited a slow retinal degeneration (Fig. 6E,F,K). After 20 d, the *dgq^1; NinaE^{PP100}* and *arr2^{Y20STOP} NinaE^{PP100}* double mutants exhibited massive photoreceptor cell death (Fig. 6I,H, respectively) relative to an equivalent aged wild-type retina (Fig. 6J). Surprisingly, the *dgq^1; arr2^{Y20STOP} NinaE^{PP100}* triple mutant exhibited only very minor rhabdomeric abnormalities after 40 d (Fig. 6G). The absence of significant cell death in this 40-d-old triple mutant relative to either of the 20-d-old double mutants and the minor suppression of *NinaE^{PP100}* degeneration by the *norpA^{P24}* and *trp^{301}* mutants revealed that both the ARR2 and $G_q\alpha$ proteins, but not activation of the light-sensitive channels, play major roles in the rapid *NinaE^{PP100}*-dependent retinal degeneration.

Figure 6. The rapid *NinaE^{pp100}* degeneration requires both the ARR2 and $G_q\alpha$ proteins. Wild-type (Oregon-R; *A, J*), *NinaE^{PP100}* (*D*), *arr2^{Y20STOP}* (*B*), *dgq^1* (*C*), *arr2^{Y20STOP} NinaE^{PP100}* (*E, H*), *dgq^1; NinaE^{PP100}* (*F, I*), and *dgq^1; arr2^{Y20STOP} NinaE^{PP100}* (*G*) flies were raised for 4 d (*B, D, E*), 10 d (*A, C, F*), 20 d (*H, I*), or 40 d (*G, J*) sectioned and examined by electron microscopy. Although both the *arr2^{Y20STOP}* and *dgq^1* mutants exhibit smaller, disorganized and occasional missing rhabdomeres relative to wild type, they are significantly more intact than the *NinaE^{pp100}* mutant. Both *arr2^{Y20STOP} NinaE^{PP100}* and *dgq^1; NinaE^{PP100}* exhibit less rhabdomere loss and photoreceptor degeneration than *NinaE^{PP100}* at 4 and 10 d, respectively. Whereas *arr2^{Y20STOP} NinaE^{PP100}* and *dgq^1; NinaE^{PP100}* possess massive degeneration at 20 d, the *dgq^1; arr2^{Y20STOP} NinaE^{PP100}* triple mutant exhibits only very minor abnormalities in the rhabdomere. Scale bar (in *A*): *A–J*, 1 μm. *K*, The time course of deep pseudopupil loss of various genotypes [*NinaE^{PP100}* flies (squares), *dgq^1* flies (circles), and *dgq^1; NinaE^{PP100}* double mutants (triangles)] raised in either constant light or constant darkness (open and filled symbols, respectively). The percentages of flies retaining a deep pseudopupil on each day were plotted against their age, with each symbol representing the average from four independent trials of 100 –150 flies per trial.

The dominant NINAE^{PP100} protein causes a constitutive disassociation and translocation of the heterotrimeric G-protein

Whole-cell recordings revealed that the *NinaE^{PP100}* mutant photoreceptors were constitutively active (Fig. 5B,D), but the weak
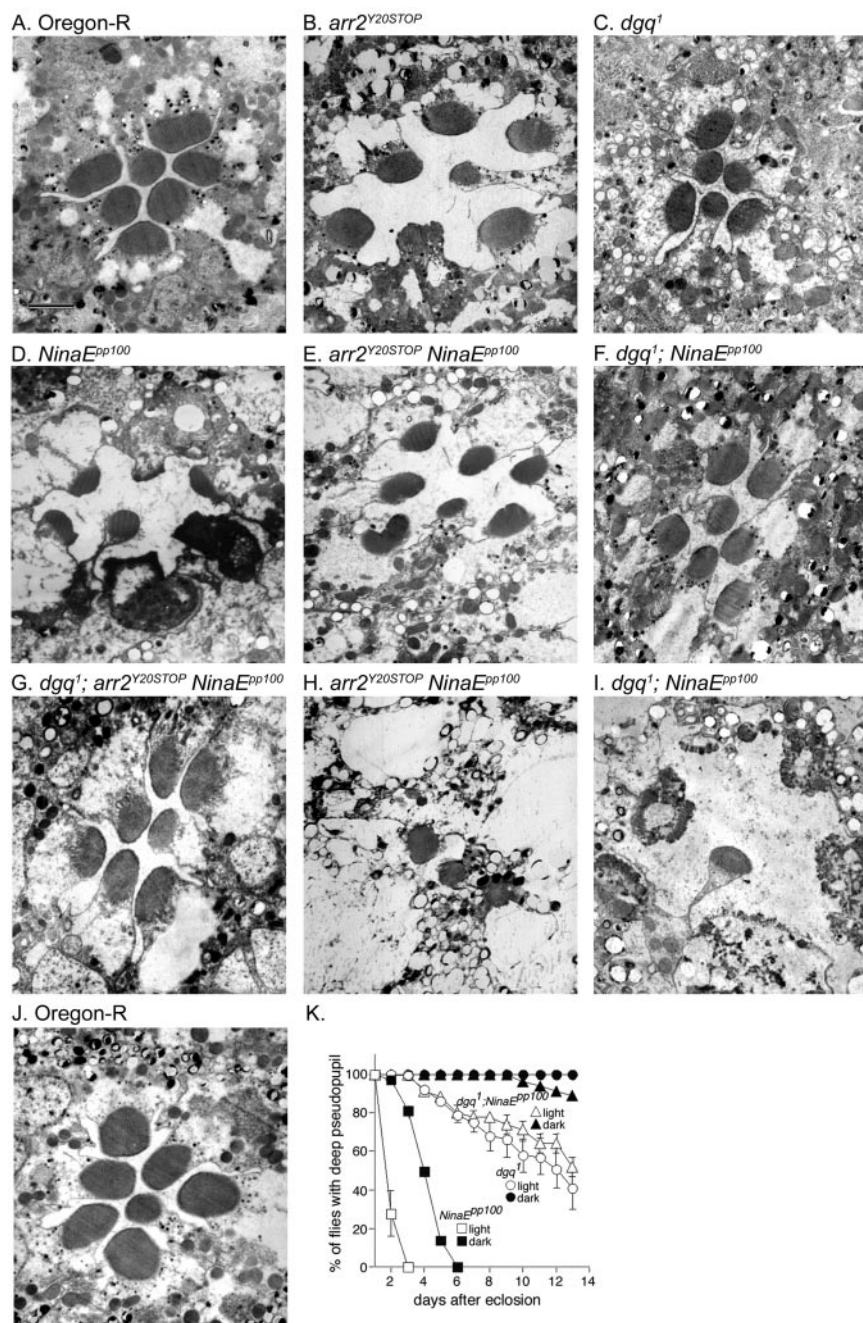
suppression of the *NinaE^{PP100}*-dependent retinal degeneration by *norpA* or *trp* suggested that constitutive activation of the light-sensitive channels was not required for the rapid *NinaE^{PP100}*-dependent retinal degeneration. We examined the extent of the constitutive activation by comparing the GTPase activity in wild-
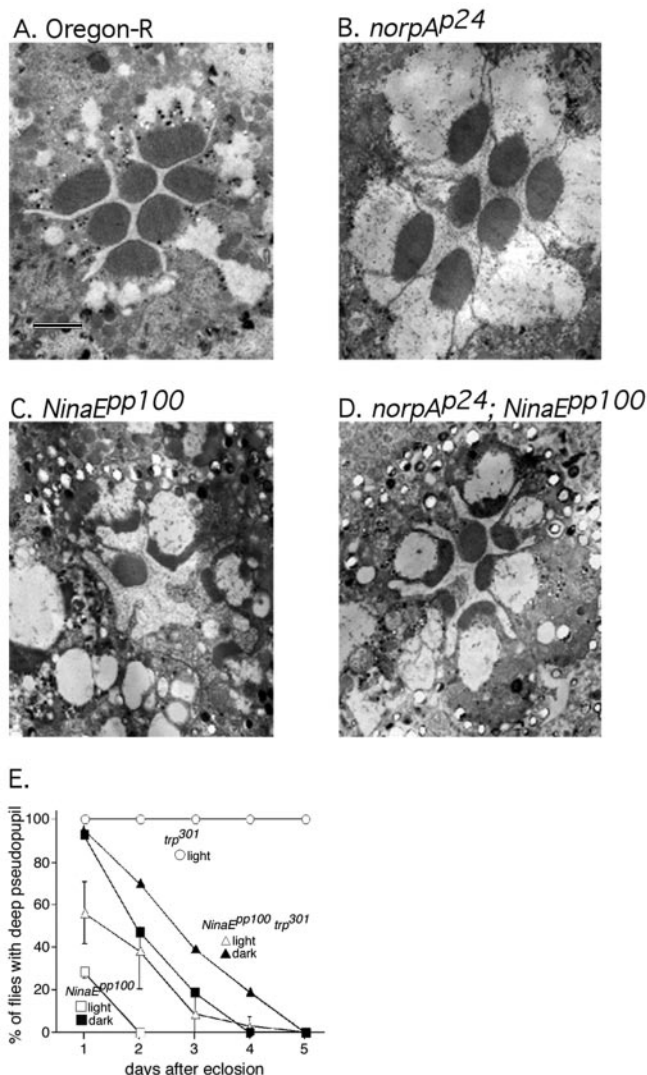
A. Oregon-R

B. *norpA^p24*

C. *NinaE^pp100*

D. *norpA^p24; NinaE^pp100*

E.

Figure 7. The *norpA^p24* and *trp^301* mutations only weakly suppress the rapid *NinaE^pp100* retinal degeneration. Wild-type (Oregon-R; *A*), *norpA^p24* (*B*), *NinaE^pp100* (*C*), and *norpA^p24; NinaE^pp100* (*D*) flies were raised for either 10 d (*A*) or 6 d (*B–D*), sectioned, and examined by electron microscopy. Although the *norpA^p24; NinaE^pp100* double mutant exhibits rhabdomere shrinkage and disruption of the cell body relative to *norpA^p24*, it lacks the massive cell degeneration characteristics observed in *NinaE^pp100*. Scale bar (in *A*): *A–D*, 1 μm. *E*, The time course of deep pseudopupil loss of various genotypes [*NinaE^pp100* flies (squares), *trp^301* flies (circles), and *NinaE^pp100 trp^301* (triangles)] raised in either constant light or constant darkness (open and filled symbols, respectively). The percentages of flies retaining a deep pseudopupil on each day were plotted against their age, with each symbol representing the average from four independent trials of 100–150 flies per trial.

type and *NinaE^pp100* mutant flies. Whereas we found high levels of light-dependent GTPase activity in wild-type flies, significantly lower light-dependent GTPase activity levels were measured in the *NinaE^pp100* mutant (Fig. 8*A*), which suggested that a large fraction of the $G_q\alpha$-protein was not activated in the *NinaE^pp100* mutant. We demonstrated previously that the $G_q\alpha$-protein translocates from the rhabdomeric membrane to the cytosol during blue light illumination (Kosloff et al., 2003). Therefore, we examined whether the $G_q\alpha$-protein in the constitutively active *NinaE^pp100* mutant photoreceptors was predominantly in the cytosol. In wild-type flies, ~80% of the $G_q\alpha$ was associated with the membrane fraction in the dark (Fig. 8*B*), which represented the GDP-bound $G_q\alpha$ in the heterotrimer. During illumination, ~70% of the $G_q\alpha$ translocated into the cytosol (Fig. 8*B*). In contrast,
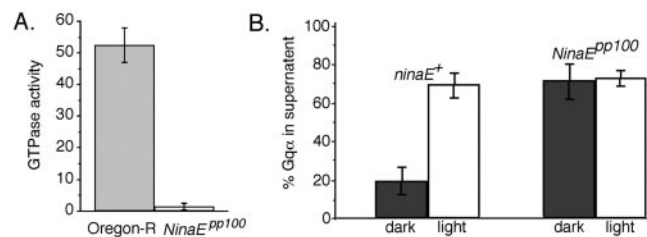
A.

B.

Figure 8. The subcellular distribution of the $G_q\alpha$-protein is altered in the *NinaE^pp100* mutant relative to wild type. *A*, The light-dependent GTPase activity (picomoles of phosphate per milligram of total protein per minute) was determined by subtracting the GTPase activity measured during orange light illumination from the GTPase activity measured during blue light illumination in the same experiment (*n* = 4). The histogram shows negligible blue light-stimulated GTPase activity in the *NinaE^pp100* mutant relative to wild-type flies. Furthermore, both the *NinaE^pp100* mutant and wild-type flies exhibited the same low level of GTPase activity in orange light (data not shown). *B*, The subcellular distribution of the $G_q\alpha$-protein was examined in wild-type (*ninaE^+*) and *NinaE^pp100* mutant heads. The percentage of total $G_q\alpha$-protein in the supernatant was determined in both light and dark conditions by subcellular fractionation and immunoblots. Although light treatment induced the translocation of $G_q\alpha$ to the cytosol in wild-type flies, light did not alter the percentage of $G_q\alpha$-protein in the *NinaE^pp100* supernatant (*n* = 4). Furthermore, the stable percentage of $G_q\alpha$ in the *NinaE^pp100* supernatant was equivalent to the percentage of $G_q\alpha$ in the light-stimulated wild-type supernatant.

~70% of the $G_q\alpha$ was present in the cytosol of the *NinaE^pp100* mutant, regardless of illumination (Fig. 8*B*). This persistent and abnormal distribution of the $G_q\alpha$-protein in the cytosol could partially account for both the absence of light-dependent GTPase activity and the desensitization of the *NinaE^pp100* mutant photoreceptor cell.

The formation of a stable rhodopsin–arrestin complex is required for the rapid photoreceptor degeneration
The ability of the *arr2^Y20STOP* mutation to significantly reduce the desensitization of the *NinaE^pp100* photoreceptor and suppress the *NinaE^pp100* degeneration suggested that the ARR2 protein persistently bound the NINAE^PP100 mutant protein (Alloway et al., 2000; Kiselev et al., 2000). ARR2 is predominantly a soluble protein when rhodopsin is not photoactivated (such as during or after orange light illumination) (Fig. 9). However, during blue light conversion of rhodopsin to metarhodopsin, ~80% of ARR2 protein binds metarhodopsin in the membrane (Fig. 9) (Byk et al., 1993). The ARR2 binding to the membrane is rhodopsin dependent, because only low levels of ARR2 are detected in *ninaE^I17* null mutant membrane fractions under either light condition (Fig. 9). In contrast, a significant percentage of ARR2 remained associated with the *NinaE^pp100* membrane, regardless of the light conditions (Fig. 9). The lower percentage of ARR2 in the newly enclosed *NinaE^pp100* membrane relative to the wild-type membrane after blue light illumination is consistent with the ~80% reduction of NINAE protein in the *NinaE^pp100* mutant compared with wild type (Fig. 1*F*). Thus, the role of ARR2 in the rapid degeneration and strong desensitization in the *NinaE^pp100* mutant is through its persistent binding to NINAE^PP100.

The *NinaE^pp100* mutant degenerates through two independent pathways that involve the abnormal distribution of the ARR2 and $G_q\alpha$
Because both the *dgq^1* and *arr2^Y20STOP* mutations significantly suppressed the rapid *NinaE^pp100*-dependent retinal degeneration (Fig. 6), we examined whether the $G_q\alpha$-protein was required for the persistent association of ARR2 with the NINAE^PP100 protein. We found that the percentage of ARR2 protein present in the membrane fraction of *dgq^1; NinaE^pp100* double mutants was es-
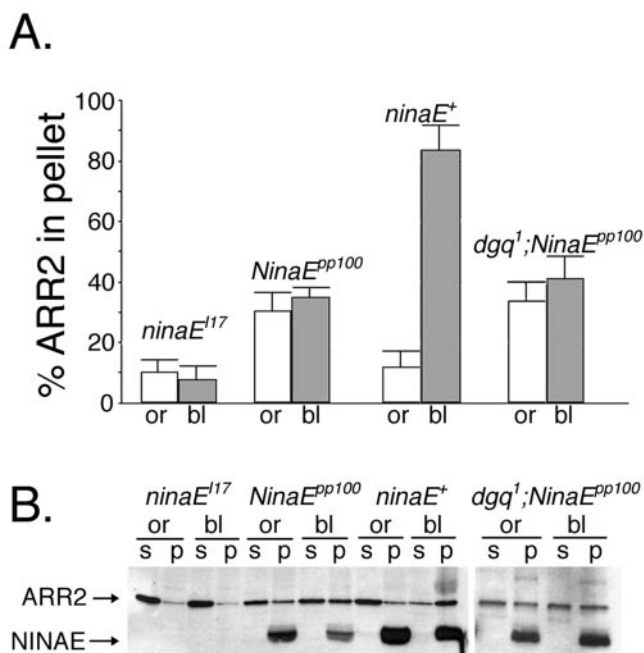
A.

B.

Figure 9. The ARR2 protein is persistently bound to the NINAE^{PP100} mutant rhodopsin. The subcellular distribution of the ARR2 protein was examined in wild-type (*ninaE*$^+$) and mutant (*ninaE*^{I17}, *NinaE*^{pp100}, and *dgq*^{1}; *NinaE*^{pp100}) heads (<4 hr after eclosion). *A*, The percentage of total ARR2 protein in the membrane pellet was determined using either 2 min of orange (or) or 2 min of blue (bl) light illumination, followed by subcellular fractionation and immunoblots (*n* = 5). The *NinaE*^{pp100} mutant had the same percentage of ARR2 protein in the pellet, regardless of the light conditions. This stable association was significantly more than that observed in the *ninaE*^{I17} null mutant and significantly less than the wild-type flies under blue light illumination. *B*, A representative immunoblot of the subcellular distribution of ARR2 and NINAE proteins in *ninaE*^{I17}, *NinaE*^{pp100}, *ninaE*$^+$, and *dgq*^{1}; *NinaE*^{pp100} fly heads. The detection of NINAE in only the membrane pellet fraction demonstrates the completeness of removing the membrane from the soluble fractions.

sentially the same as in *NinaE*^{PP100} mutant flies (Fig. 9). Because the loss of the G$_q\alpha$ protein did not reduce the level of the persistent NINAE^{PP100}–ARR2 complexes, the *dgq*^{1} suppression of *NinaE*^{PP100} degeneration must be arrestin independent. This demonstrates that G$_q\alpha$ is involved in a novel mechanism for the rapid *NinaE*^{PP100} degeneration, which may involve its predominant and persistent localization in the cytosol. Furthermore, the complete suppression observed in the 40-d-old *dgq*^{1}; *arr2*^{Y20STOP} *NinaE*^{PP100} triple mutant clearly demonstrates that both the G$_q\alpha$ and ARR2-dependent degeneration pathways are both necessary and sufficient to account for the entire *NinaE*^{PP100}-dependent degeneration process.

Discussion

The *NinaE*^{PP100} mutant exhibits a novel retinal degeneration phenotype

We isolated a novel dominant rhodopsin mutation, *NinaE*^{PP100}, that requires the presence of both G$_q\alpha$ and arrestin to induce a rapid degeneration. Transgenic expression of an *in vitro*-generated glycine-to-arginine mutation at position 299 conclusively demonstrated that this is the molecular cause of the dominant *NinaE*^{PP100} mutant phenotype (Fig. 2C). Previously, several dominant rhodopsin mutations were isolated that blocked rhodopsin trafficking and maturation out of the endoplasmic reticulum and slowly degenerated (Colley et al., 1995; Kurada and O'Tousa, 1995; Kurada et al., 1998). Several lines of data demonstrated that the *NinaE*^{PP100} mutation did not affect rhodopsin

trafficking and maturation. First, the *ninaE*^{D1} mutation, which is one of the most severe of the previously isolated dominant rhodopsin mutations (Kurada and O'Tousa, 1995; Kurada et al., 1998), suppressed the rapid *NinaE*^{PP100} degeneration (Fig. 3). Therefore, the NINAE^{PP100} protein must exert its effect subsequent to the *ninaE*^{D1} trafficking defect. Second, *NinaE*^{PP100}/*ninaE*$^+$ flies lacked immature forms of rhodopsin on immunoblots (Fig. 1F). Thus, both wild-type and NINAE^{PP100} mutant proteins must complete their maturation, although the NINAE^{PP100} protein was present at ~20% of the NINAE$^+$ protein level (Fig. 1F). Third, electron microscopy independently immunolocalized both epitope-tagged NINAE$^+$ and epitope-tagged NINAE^{PP100} in the rhabdomeres of *NinaE*^{PP100}/*ninaE*$^+$ flies (data not shown), which confirmed that both forms reach the rhabdomere. Therefore, *NinaE*^{PP100} represents a new *Drosophila* model for dominant rhodopsin mutations.

The mechanisms underlying the highly reduced sensitivity to light in the *NinaE*^{PP100} mutant and its implications on congenital night blindness (CNB) in humans

The strongly desensitized *NinaE*^{PP100} photoreceptor was characterized by the following: (1) the intense light required to elicit a small-amplitude response that lacked the typical bump noise (Fig. 4A), (2) the increased light intensity necessary to reach the saturated amplitude (Fig. 4B), and (3) the shift of the intensity–response relationship toward higher light intensity levels (Figs. 4B, 5A). Although either the 80% decrease in the number of rhodopsin molecules (Fig. 1F) or the 80% decrease of G$_q\alpha$-protein associated with the membrane (Fig. 8B) would reduce the *NinaE*^{PP100} light sensitivity, they are insufficient to account for the observed four orders of magnitude reduction. A more significant mechanism is the constant state of light adaptation that results from the persistent NINAE^{PP100}–ARR2 complex (Fig. 9). Normally, rhodopsin is present at a 5:1 molar ratio to ARR2 (Dolph et al., 1993). However, the NINAE^{PP100} mutant protein is expressed at only 20% of the wild-type level of rhodopsin in wild-type photoreceptors (Fig. 1F), which yields an ~1:1 molar ratio with ARR2. Thus, if 30–40% of the ARR2 is associated with the *NinaE*^{PP100} membrane, approximately an equivalent percentage of the NINAE^{PP100} mutant protein is likely in a NINAE^{PP100}–ARR2 complex. This would correspond to ~35% of the NINAE^{PP100} being present in the persistent complex, which corresponds to 6–8% of the rhodopsin level in wild-type photoreceptors. This complex could account for the shift in the intensity–response curve toward brighter light (Fig. 5A). The fact that the light response in a fraction of mutant cells reached a normal peak amplitude at intense lights (Fig. 4B) is consistent with a significant number of light-sensitive rhodopsin molecules (i.e., ~10^3-10^5) (Johnson and Pak, 1986) not being bound by arrestin. The NINAE^{PP100}–ARR2 complex would also account for the minimal light-stimulated GTPase activity in the *NinaE*^{PP100} mutant photoreceptor cell. However, genetic elimination of ARR2 only partially increased the light sensitivity of the mutant *NinaE*^{PP100} (Figs. 4A, 5A), which could be explained by two different mechanisms. First, constitutively active NINAE^{PP100} would continually open the light-sensitive channels (Fig. 5), which leads to a persistent Ca^{2+} influx and photoreceptor desensitization. Second, activated G$_q\alpha$-protein may stimulate the internalization of specific G-protein-coupled receptors in the absence of arrestin binding (Rochdi and Parent, 2003). Thus, constitutively active NINAE^{PP100} would activate G$_q\alpha$, which could drive internalization of both wild-type and NINAE^{PP100} rhodopsin molecules to desensitize the photoreceptor cell.

This strong desensitization response, with only a minor effect on retinal degeneration, is similar to the human CNB phenotype (Dryja, 2000). One form of autosomal dominant CNB results from constitutively active forms of rod opsin (Jin et al., 2003). Three dominant rod opsin mutations were shown to cause a significant shift in the intensity–response relationship of transgenic *Xenopus* rods (Jin et al., 2003). The constitutive activity and desensitization observed in the $NinaE^{PP100}$ mutant suggests that the $NINAE^{PP100}$ mutant rhodopsin may serve as an important model for elucidating the molecular details of one form of autosomal dominant CNB.

A novel mechanism for dominant rhodopsin-mediated retinal degeneration

The $NinaE^{PP100}$ dominant mutation induces three different degeneration mechanisms. The first involves constitutive opening of the light-sensitive channels. The *Drosophila* $rdgA^{BS12}$ and trp^{P365} mutations were shown to constitutively depolarize the photoreceptor cell and cause retinal degeneration (Raghu et al., 2000; Yoon et al., 2000). Furthermore, three different *trp* alleles (including trp^{301}) significantly slowed the rapid $rdgA^{BS12}$ retinal degeneration, which confirmed that the $rdgA^{BS12}$ degeneration was dependent on the constitutive opening of the light-activated channels (Raghu et al., 2000). However, the constitutive current observed in the $NinaE^{PP100}$ mutant was approximately fivefold smaller than that found in the *Drosophila* $rdgA^{BS12}$ and trp^{P365} mutants (Raghu et al., 2000; Yoon et al., 2000) and was not found in all of the cells (Fig. 5B). Furthermore, the weak suppression by the $norpA^{24}$ and trp^{301} mutations on the rapid $NinaE^{PP100}$ degeneration (Fig. 7 D,E, respectively) confirmed that the constitutive opening of the light-sensitive channels is a minor $NinaE^{PP100}$ degeneration mechanism.

The second degeneration mechanism involves the formation of a stable $NINAE^{PP100}$–ARR2 complex. A variety of *Drosophila* mutations were shown previously to induce retinal degeneration by generating a stable NINAE–ARR2 complex that was endocytosed in a clathrin-dependent manner (Alloway et al., 2000; Kiselev et al., 2000). However, $NinaE^{PP100}$ is the first *Drosophila* rhodopsin mutation that persistently targeted ARR2 to the membrane in all light conditions (Fig. 9). On the basis of the $arr2^{Y20STOP}$ mutation suppressing the $NinaE^{PP100}$ degeneration (Fig. 6), the $NINAE^{PP100}$–ARR2 complex accounts for a major $NinaE^{PP100}$ degeneration mechanism. The K296E opsin mutation in transgenic mice exhibited an analogous dominant photoreceptor degeneration phenotype (Robinson et al., 1992; Li et al., 1995; Rim and Oprian, 1995). Although the K296E mutant opsin constitutively activated the heterotrimeric G-protein in cell culture, it failed to constitutively stimulate the phototransduction cascade in the mouse photoreceptor because it was persistently phosphorylated and bound by arrestin. This stable rhodopsin–arrestin complex may be a common stimulator of photoreceptor apoptosis for constitutively active rhodopsin mutations rather than persistent activation of the phototransduction cascade.

The third and novel *Drosophila* degeneration mechanism requires $G_q\alpha$ but not activation of the visual transduction cascade, because neither the $norpA^{p24}$ nor trp^{301} mutations suppressed $NinaE^{PP100}$ degeneration to the same extent as dgq^1 (Figs. 7, 6, respectively). Furthermore, the inability of the dgq^1 mutation to disrupt the stable $NINAE^{PP100}$–ARR2 complex (Fig. 9) and the consistent presence of 70% of the $G_q\alpha$-protein in the cytosolic fraction of both $NinaE^{PP100}$ and $arr2^{Y20STOP}$ $NinaE^{PP100}$ mutants (Fig. 8 B and data not shown, respectively) demonstrated that the $G_q\alpha$- and ARR2-dependent degeneration mechanisms were in-

dependent. The light-independent localization of most of the $G_q\alpha$-protein to the $NinaE^{PP100}$ cytosol is consistent with the constitutively active $NINAE^{PP100}$ stimulating $G_q\alpha$ dissociation from $G\beta\gamma$ and the subsequent depalmitoylation of $G_q\alpha$ (Kosloff et al., 2003). The cytosolic localization and the markedly decreased light-dependent GTPase activity in the $NinaE^{PP100}$ mutant (Fig. 8) suggests that the $NINAE^{PP100}$ protein either diminishes the interaction between the cytosolic $G_q\alpha$-GTP with the membrane-associated *norpA*-encoded phospholipase C effector molecule, which also functions as a GTPase activating protein (Cook et al., 2000), or suppresses the reassociation of the cytosolic $G_q\alpha$ with the membrane. Because the loss of $G_q\alpha$-protein significantly slowed the $NinaE^{PP100}$ degeneration, the persistent cytosolic localization of $G_q\alpha$ induces the degeneration rather than its absence from the membrane.

Whereas most previously characterized retinal degeneration models identified a single major pathway, the $NinaE^{PP100}$ mutant identified two major degeneration mechanisms, the stable $NINAE^{PP100}$–ARR2 complex and the $G_q\alpha$-dependent pathway. The ability of $ninaE^{D1}$ to prevent the rapid $NinaE^{PP100}$-dependent degeneration (Fig. 3) is consistent with the requirement of $NINAE^{PP100}$ to reach the rhabdomere and interact with the ARR2 and $G_q\alpha$ proteins. Recently, knock-out mice revealed that light-induced degeneration also involved two mechanisms (Hao et al., 2002), one requiring the transducin α subunit and the other involving photoactivated metarhodopsin and/or its bleaching intermediates (Hao et al., 2002). Thus, the $NinaE^{PP100}$ mutant may reveal not only the complex interactions between constitutive activation and desensitization but also the multiplicity of mechanisms that may be involved in some of the rhodopsin-dependent degeneration mutations.

References

Alloway PG, Dolph PJ (1999) A role for the light-dependent phosphorylation of visual arrestin. Proc Natl Acad Sci USA 96:6072–6077.

Alloway PG, Howard L, Dolph PJ (2000) The formation of stable rhodopsin-arrestin complexes induces apoptosis and photoreceptor cell degeneration. Neuron 28:129–138.

Ashburner M (1989) *Drosophila*: a laboratory manual. Cold Spring Harbor, NY: Cold Spring Harbor Laboratory.

Blumenfeld A, Erusalimsky J, Heichal O, Selinger Z, Minke B (1985) Light-activated guanosinetriphosphate in *Musca* eye membranes resembles the prolonged depolarizing afterpotential in photoreceptor cells. Proc Natl Acad Sci USA 82:7116–7121.

Byk T, Bar-Yaacov M, Doza YN, Minke B, Selinger Z (1993) Regulatory arrestin cycle secures the fidelity and maintenance of the fly photoreceptor cell. Proc Natl Acad Sci USA 90:1907–1911.

Colley NJ, Cassil JA, Baker EK, Zuker CS (1995) Defective intracellular transport is the molecular basis of rhodopsin-dependent dominant retinal degeneration. Proc Natl Acad Sci USA 92:3070–3074.

Cook B, Bar-Yaacov M, Cohen Ben-Ami H, Goldstein RE, Paroush Z, Selinger Z, Minke B (2000) Phospholipase C and termination of G-protein-mediated signaling *in vivo*. Nat Cell Biol 2:296–301.

Dolph PJ, Ranganathan R, Colley NJ, Hardy RW, Socolich M, Zuker CS (1993) Arrestin functions in inactivation of G protein-coupled receptor rhodopsin *in vivo*. Science 260:1910–1915.

Dryja TP (2000) Molecular genetics of Oguchi disease, fundus albipunctatus, and other forms of stationary night blindness: LVII Edward Jackson Memorial Lecture. Am J Ophthalmol 130:547–563.

Dryja TP, Berson EL, Rao VR, Oprian DD (1993) Heterozygous missense mutation in the rhodopsin gene as a cause of congenital stationary night blindness. Nat Genet 4:280–282.

Franceschini N (1972) Pupil and pseudopupil in the compound eye of *Drosophila*. In: Information processing in the visual systems of arthropods (Wehner R, ed), pp 75–82. Berlin: Springer.

Gal A, Apfelstedt-Sylla E, Janecke AR, Zrenner Z (1997) Rhodopsin mutations in inherited dystrophies and dysfunctions. Prog Ret Eye Res 16:51–79.

Hao W, Wenzel A, Obin MS, Chen CK, Brill E, Krasnoperova NV, Eversole-

Cire P, Kleyner Y, Taylor A, Simon MI, Grimm C, Reme CE, Lem J (2002) Evidence for two apoptotic pathways in light-dependent retinal degeneration. Nat Genet 32:254–260.

Hardie RC (1991) Voltage-sensitive potassium channels in *Drosophila* photoreceptors. J Neurosci 11:3079–3095.

Hardie RC, Minke B (1992) The *trp* gene is essential for a light-activated Ca^{2+} channel in *Drosophila* photoreceptors. Neuron 8:643–651.

Hardie RC, Minke B (1994) Spontaneous activation of light-sensitive channels in *Drosophila* photoreceptors. J Gen Physiol 103:389–407.

Hillman P, Hochstein S, Minke B (1983) Transduction in invertebrate photoreceptors: role of pigment bistability. Physiol Rev 63:668–772.

Jin S, Cornwall MC, Oprian DD (2003) Opsin activation as a cause of congenital night blindness. Nat Neurosci 6:731–735.

Johnson EC, Pak WL (1986) Electrophysiological study of *Drosophila* rhodopsin mutants. J Gen Physiol 88:651–673.

Kaushal S, Khorana HG (1994) Structure and function in rhodopsin. 7. Point mutations associated with autosomal dominant retinitis pigmentosa. Biochemistry 33:6121–6128.

Kiselev A, Subramaniam S (1994) Activation and regeneration of rhodopsin in the insect visual cycle. Science 266:1369–1373.

Kiselev A, Socolich M, Vinos J, Hardy RW, Zuker CS, Ranganathan R (2000) A molecular pathway for light-dependent photoreceptor apoptosis in *Drosophila*. Neuron 28:139–152.

Kosloff M, Elia N, Joel-Almagor T, Timberg R, Zars TD, Hyde DR, Minke B, Selinger Z (2003) Regulation of light-dependent Gqalpha translocation and morphological changes in fly photoreceptors. EMBO J 22:459–468.

Kurada P, O'Tousa JE (1995) Retinal degeneration caused by dominant rhodopsin mutations in *Drosophila*. Neuron 14:571–579.

Kurada P, Tonini TD, Serikaku MA, Piccini JP, O'Tousa JE (1998) Rhodopsin maturation antagonized by dominant rhodopsin mutants. Vis Neurosci 15:693–700.

Lee Y-J, Dobbs MB, Verardi ML, Hyde DR (1990) *dgq*: a *Drosophila* gene encoding a visual system-specific G alpha molecule. Neuron 5:889–898.

Lee Y-J, Shah S, Suzuki E, Zars T, O'Day PM, Hyde DR (1994) The *Drosophila dgq* gene encodes a G alpha protein that mediates phototransduction. Neuron 13:1143–1157.

Leonard DS, Bowman VD, Ready DF, Pak WL (1992) Degeneration of photoreceptors in rhodopsin mutants of *Drosophila*. J Neurobiol 23:605–626.

Lewis EB, Bacher F (1968) Method of feeding ethyl methane sulfonate (EMS) to *Drosophila* males. Dros Inf Serv 43:193.

Li T, Franson W, Gordon JW, Berson EL, Dryja TP (1995) Constitutive activation of phototransduction is not a cause of photoreceptor degeneration. Proc Natl Acad Sci USA 92:3551–3555.

Milligan S, Alb JG, Elagina RB, Bankaitis VA, Hyde DR (1997) The phosphatidylinositol transfer protein domain of *Drosophila* Retinal Degeneration B protein is essential for photoreceptor cell survival and recovery from light stimulation. J Cell Biol 139:351–363.

Min KC, Zvyaga TA, Cypess AM, Sakmar TP (1993) Characterization of mutant rhodopsins responsible for autosomal dominant retinitis pigmentosa. Mutations on the cytoplasmic surface affect transducin activation. J Biol Chem 268:9400–9404.

Minke B, Hardie RC (2000) Genetic dissection of *Drosophila* phototransduction. In: Molecular mechanisms in visual transduction (Stavenga DG, van der Hope DJN, Pugh E, eds), pp 449–525. North Holland, The Netherlands: Elsevier.

O'Tousa JE, Baehr W, Martin RL, Hirsh J, Pak WL, Applebury ML (1985) The *Drosophila ninaE* gene encodes an opsin. Cell 40:839–850.

Paetkau DW, Elagin VA, Sendi LM, Hyde DR (1999) Isolation and characterization of *Drosophila* retinal degeneration B suppressors. Genetics 151:713–724.

Peretz A, Suss-Toby E, Rom-Glas A, Arnon A, Payne R, Minke B (1994) The light response of *Drosophila* photoreceptors is accompanied by an increase in cellular calcium: effects of specific mutations. Neuron 6:1257–1267.

Phelan JK, Bok D (2000) A brief review of retinitis pigmentosa and the identified retinitis pigmentosa genes. Mol Vis 6:116–124.

Raghu P, Usher K, Jonas S, Chyb S, Polyanovsky A, Hardie RC (2000) Constitutive activity of the light-sensitive channels TRP and TRPL in the *Drosophila* diacylglycerol kinase mutant, *rdgA*. Neuron 26:169–179.

Rao VR, Cohen GB, Oprian DD (1994) Rhodopsin mutation G90D and a molecular mechanism for congenital night blindness. Nature 367:639–642.

Rattner A, Sun H, Nathans J (1999) Molecular genetics of human retinal disease. Annu Rev Genet 33:89–131.

Rim J, Oprian DD (1995) Constitutive activation of opsin: interaction of mutants with rhodopsin kinase and arrestin. Biochemistry 34:11938–11945.

Robinson PR, Cohen GB, Zhukovsky EA, Oprian DD (1992) Constitutively active mutants of rhodopsin. Neuron 9:719–725.

Rochdi MD, Parent JL (2003) Gαq-coupled receptor internalization specifically induced by Gαq signaling. J Biol Chem 278:17827–17837.

Roof DJ, Adamian M, Hayes A (1994) Rhodopsin accumulation at abnormal sites in retinas of mice with a human P23H rhodopsin transgene. Invest Ophtalmol Vis Sci 35:4049–4061.

Scott K, Becker A, Sun Y, Hardy R, Zuker CS (1995) Gq alpha protein function *in vivo*: genetic dissection of its role in photoreceptor cell physiology. Neuron 15:919–927.

Shetty KM, Kurada P, O'Tousa JE (1998) Rab6 regulation of rhodopsin transport. J Biol Chem 273:20425–20430.

Spradling AC (1986) P element-mediated transformation. In: *Drosophila* a practical approach (Roberts DB, ed), pp 175–196. Oxford: IRL.

Sung C-H, Makino C, Baylor D, Nathans J (1994) A rhodopsin gene mutation responsible for autosomal dominant retinitis pigmentosa results in a protein that is defective in localization to the photoreceptor outer segment. J Neurosci 14:5818–5833.

Vihtelic TS, Hyde DR, O'Tousa JE (1991) Isolation and characterization of the *Drosophila* retinal degeneration B (*rdgB*) gene. Genetics 127:761–768.

Vihtelic TS, Goebl M, Milligan S, O'Tousa JE, Hyde DR (1993) Localization of *Drosophila* retinal degeneration B, a membrane-associated phosphatidylinositol transfer protein. J Cell Biol 122:1013–1022.

Wang Q, Chen Q, Zhao K, Wang L, Traboulsi EI (2001) Update on the molecular genetics of retinitis pigmentosa. Ophthalmic Genet 22:133–154.

Yoon J, Ben-Ami HC, Hong YS, Park S, Strong LLR, Bowman J, Geng C, Baek K, Minke B, Pak WL (2000) Novel mechanism of massive photoreceptor degeneration caused by mutation in the *trp* gene of *Drosophila*. J Neurosci 20:649–659.

Zuker CS, Cowman AF, Rubin GM (1985) Isolation and structure of a rhodopsin gene from *D. melanogaster*. Cell 40:851–858.